Vibrational-rotational distributions of NO formed from N + O_2 reactive collisions

B. Ramachandran*
Chemistry, P.O. Box 10348, Louisiana Tech University, Ruston, LA 71272, USA

N. Balakrishnan† and A. Dalgarno‡
Institute for Theoretical Atomic and Molecular Physics, Harvard-Smithsonian Center for Astrophysics, Cambridge, MA 02138, USA

Abstract

We present the results of quasiclassical trajectory calculations for the N(^4S) + O_2 reaction over a broad range of collision energies with scaled *ab initio* potential energy surfaces of the $^2A'$ and $^4A'$ electronic states. The analysis of product rovibrational distributions supports the suggestion that this reaction is a source of highly excited NO in the upper atmosphere. The computed NO vibrational distribution is found to be in good agreement with a recent measurement.

*E-mail: ramu@chem.latech.edu

†E-mail: nbala@cfa.harvard.edu

‡E-mail: adalgarno@cfa.harvard.edu

1 Introduction

The observation of highly rovibrationally excited NO in the lower thermosphere by the CIRRIS 1A Space Shuttle experiment [1,2] has given rise to much interest in the chemistry of NO and its abundance in the upper atmosphere. The formation of NO in the upper atmosphere occurs through the following elementary reactions which constitute the Zeldovich mechanism [3]:

$$\mathrm{O}(^3P) + \mathrm{N_2} \rightarrow \mathrm{NO} + \mathrm{N}, \quad (1)$$

$$\mathrm{N}(^4S) + \mathrm{O_2} \rightarrow \mathrm{NO} + \mathrm{O}. \quad (2)$$

Of these, the first reaction is highly endothermic ($\Delta H_0^\circ \simeq 318$ kJ/mol) while the second is highly exothermic ($\Delta H_0^\circ \simeq -133$ kJ/mol). Reaction (1) is not expected to be an important source of NO in the atmosphere under thermal conditions but the presence of energetic oxygen atoms and vibrationally excited N_2 may induce reactivity. The reaction of electronically excited $\mathrm{N}(^2D)$ atoms with O_2 also contributes to NO production, especially in the lower thermosphere. Here we focus on reaction (2) which has been suggested [4] as the source of the highly rovibrationally excited NO observed in the CIRRIS 1A experiments.

Despite the large exothermicity associated with reaction (2) it is slow at room temperature and requires an activation energy of about 0.3 eV. Hence energetic $\mathrm{N}(^4S)$ atoms are required for the reaction (2) to proceed efficiently. The importance of energetic $\mathrm{N}(^4S)$ atoms as a source NO in the thermosphere has become a topic of considerable interest because superthermal $\mathrm{N}(^4S)$ atoms are produced in the thermosphere by a variety of processes [5,6]. Due to the high exothermicity of (2) and the involvement of energetic $\mathrm{N}(^4S)$ atoms, the product NO is expected to be formed with significant vibrational and rotational excitation. Infrared emission from rovibrationally excited NO has long been known to be an important cooling mechanism in the terrestrial thermosphere.

Laboratory investigations of the $\mathrm{N}(^4S) + \mathrm{O_2}$ reaction have provided thermal rate constants over a wide range of temperatures [7–9] but data on NO vibrational distributions have been rather limited [10–14]. Measurement of product vibrational distributions in the reaction is complicated by the rapid vibrational quenching of excited NO molecules by O_2. Theoretical studies of this reaction have focused on the calculation of thermal rate constants [15–21] and product vibrational

distributions [17, 19]. The investigations by Gilibert et al. [15] used a potential energy surface that has an unphysical barrier in the entrance channel giving rise to an activation energy that is about 0.2 eV higher than the experimentally determined value of 0.3 eV. Bose and Candler [19] have reported product NO vibrational distributions but at temperatures that typically exist in hot plasmas.

In this Letter, we report the results of quasiclassical trajectory (QCT) calculations on the $N(^4S)$ + O_2 reaction using the potential surfaces of Duff et al. [16] for the $^2A'$ and the $^4A'$ electronic states. The goal of this study is to examine the NO rotational distributions in the various vibrational levels populated as a result of the reaction at the ambient temperatures of the thermosphere.

2 Calculations

Three electronic states arise from the combination of the reactants $N(^4S_u)$ + $O_2(X\ ^3\Sigma_g^-)$, namely, $^2A'$, $^4A'$ and $^6A'$. Of these, $^2A'$ and $^4A'$ states correlate with the products $NO(X\ ^2\Pi)$ + $O(^3P_g)$, and the $^6A'$ state correlates with product states that lie at much higher energy. This study makes use of the potential surfaces for the $^2A'$ and $^4A'$ states obtained by Duff et al. [16] by fitting adjusted *ab initio* energies of Walch and Jaffe [22]. The adjustments were aimed at reproducing the reaction barriers estimated from experimental data. The reaction barriers are 0.30 eV on the $^2A'$ surface and 0.65 eV on the $^4A'$ surface. The potential well corresponding to the NO_2 molecule lies on the $^2A'$ surface, on the product side of the reaction barrier. Although the potential surface is known to be inaccurate in the vicinity of the NO_2 equilibrium geometry, it is not expected to seriously affect studies of the N + O_2 reaction since the total energy available to the system to surmount the reaction barrier is far above that of the NO_2 minimum.

The center of mass collision energies for QCT calculations were taken to be in the range 0.3 eV to 3.0 eV. At each collision energy, at least 3,000 trajectories were initiated from the $O_2(v = 0, 1)$ states. Larger number of trajectories were used at collision energies close to the reaction threshold in order to increase the accuracy of the calculated reaction cross sections. The O_2 rotational state for each trajectory was selected randomly from a Boltzmann distribution at four temperatures: 200, 415, 742, and 1000 K. These temperatures correspond to the ambient temperatures at altitudes of 100, 120, 140 and 200 km. We have also propagated a total of 80,000 trajectories (40,000 on each electronic surface) at a fixed collision energy of 3.0 eV, which roughly corresponds to the conditions

present in the recent experiments of Caledonia et al. [14]. The rotational temperature of the O_2 in these calculations was chosen to be 1000 K, which is probably higher than that in the experiments but closer to the conditions found in the upper atmosphere.

The reaction cross-sections calculated from the $^2A'$ and $^4A'$ surfaces were found to be very similar to those obtained by Balakrishnan and Dalgarno [21] using a quantum-classical approach. As a further check on the accuracy of the QCT calculations, we calculated thermal rate coefficients from the cross-sections for each electronic state, weighted by appropriate degeneracy factors,

$$k = \frac{1}{6}k(^2A') + \frac{1}{3}k(^4A'). \tag{3}$$

These values were also found to be in close agreement with the quantum-classical results of Balakrishnan and Dalgarno [21]. The high exothermicity of this reaction allows a very large number of product vibrational levels to be populated. In each vibrational level, the rotational distribution was obtained by a binning procedure based on the rotational quantum number calculated from the rotational energy of NO. These results are presented and discussed in the following Section.

3 Results and Discussion

The NO vibrational distributions obtained from $O_2(v = 0, 1)$ by QCT calculations at a relative translational energy of 3.0 eV and an O_2 rotational temperature of 1000 K are shown in Figure 1. In combining the distributions from the two electronic surfaces, the same weights as in Eq. (3) were used. The normalization of these distributions is such that the the *sum* of the $v = 0$ and $v = 1$ curves peaks at unity. It is clear that, in keeping with the propensity rules established by Polanyi and coworkers [23], the early barriers on the two potential surfaces cause the reaction cross-section to decrease with vibrational excitation of the reactant molecule. Also, in keeping with these propensity rules, the relative translational energy of the reactants is efficiently channeled into internal energy of the products. The present vibrational distributions bear close similarity to the lower temperature results of Bose and Candler [19], including the location of the maxima of the distributions, at $v' = 2$.

The rotational distribution in the $NO(v' = 2)$ state under the same conditions as those present in Fig. 1 is shown in Figure 2. The rather large variations in the relative populations of adjacent rotational levels appear to be due, at least in part, to incomplete convergence of the distributions.

The oscillations become less pronounced as the total number of reactive trajectories increase, indicating that they are due to statistical noise, but they appear to converge at slow rate. For example, the results presented in Fig. 2 represent 41,166 reactive trajectories. Analogous results from about 20,000 trajectories are only slightly more oscillatory. A convenient way to estimate the rotational distributions that would result from an extremely large ensemble of trajectories is to smooth the distribution using, say, a sliding average of the populations of several neighboring levels. Such a smoothed distribution which weights the neighboring rotational states using a Gaussian with a HWHM of 5 is also shown in Fig. 2. The smoothed distribution is faithful to the local trends and the general shape of the distribution. The normalization in this figure is such that the maximum value of the *sum* of the smoothed distributions for $v = 0$ and $v = 1$ is unity.

Due to the large number of the vibrational and rotational states populated, it is most convenient to present the rovibrational distributions as a three-dimensional function of both v' and j'. We present two types of distributions: one type includes the rovibrational distributions at all collision energies studied, and the other shows the results for a single collision energy. A typical example of the first type is shown in Fig. 3. These distributions are smoothed in the j' direction as in Fig. 2 but no smoothing is done for the v' direction. Panels (a) and (b) respectively show the distributions resulting from the O_2 $v = 0$ and 1 states, at an O_2 rotational temperature of 742 K. The normalization is once again such that the sum of the two distributions peaks at unity. The unusually broad distributions of both vibrational and rotational quantum numbers are clearly identifiable in these figures, indicating that a large fraction of the reactant energy is channeled into the internal energy of the products.

In Figure 4, we present the rovibrational distributions resulting from $N + O_2$ collisions at a fixed relative translational energy of 3.0 eV, where the initial O_2 rotational temperature is 1000 K. The two panels of this figure are arranged and normalized in the same manner as Fig. 3. The main difference between Fig. 3 and 4, which is immediately obvious, is the sharp drop-off of the distributions at the high j' values in the latter. Similar behavior is also more clearly seen in Fig. 2 which is based on a subset of the data plotted in Fig. 4. At fixed collision energies, the highest energetically accessible product rotational state in each vibrational manifold is populated, further underscoring the efficiency with which reagent energy is channeled into the internal energy of the products.

Caledonia et al. [14] have measured the vibrationally resolved cross sections for the $N(^4S) + O_2$ reaction at a center of mass kinetic energy of 3 eV. In Fig. 5 we compare their data with our results in which the initial O_2 rotational temperature was taken to be 1000 K. Noting that the uncertainty in the experimental data is about a factor of two [14], the agreement with the experimental results is quite satisfactory. The experimental data show a dip in the production of $v' = 3$ relative to $v' = 2$ and 4 and also of $v' = 6$ relative to 5 and 7. QCT results do not reflect these oscillations but are in good agreement with those of Duff et al. [16,27].

A comparison of some of the results from the present QCT calculations with the experimental results of Caledonia et al. [14], expressed as cross sections divided by π, is presented in Table I. Also given here is the mean value of the rotational level populated for each v', calculated as

$$\langle j' \rangle_{v'} = \frac{\sum_{j'}(2j'+1)j' P_{v'j'}}{\sum_{j'}(2j'+1)P_{v'j'}}. \tag{4}$$

From the $\langle j' \rangle$ value thus obtained, a mean rotational temperature T_{rot} for NO is calculated under the assumption that for a linear molecule, $\langle \varepsilon_{rot} \rangle \simeq k_B T_{rot}$, where k_B is the Boltzmann constant. The $\langle j' \rangle$ values vary from 118 for $v' = 0$ to 17 for $v' = 24$. The corresponding rotational temperatures are in the range 1200–34000 K, which completely encompasses the range of 4000–10000 K (which corresponds to $\langle j' \rangle = 40 - 64$) used by Caledonia et al. [14] in their spectral fits. The Table also shows that the product vibrational level resolved cross-sections from the $O_2(v = 0)$ state in the present calculations are in excellent agreement with the results of Duff [27].

In summary, we confirm that at the ambient temperatures in the thermosphere the $N(^4S)$ + O_2 reaction produces NO in highly vibrationally and rotationally excited levels. However, our QCT calculations do not reflect the oscillatory behavior of the product vibrational distributions observed in the experiments [14]. Although the absolute cross-section values reported in Ref. [14] may be uncertain by a factor of 2, Caledonia et al. state that the relative values of the cross-sections should have considerably smaller errors. The disagreement would imply that the observed oscillatory behavior is due to quantum effects or due to the inaccuracies in the potential surfaces used. Since the experiments have been conducted under single-collision conditions, the collisional quenching of NO by the unreacted O_2 is not an important consideration.

Nitric oxide is also produced in the reaction of electronically excited $N(^2D)$ atoms with O_2 [24–26]. Due to the large exothermicity ($\Delta H_0^\circ \simeq -362$ kJ/mol) of this process NO is expected to be formed with high vibrational and rotational excitation. Therefore, the actual rovibrational

distribution of NO in the thermosphere will depend on the relative contribution from (2) and the $N(^2D) + O_2$ reaction [6]. Though measurements of the rate coefficient for the $N(^2D) + O_2$ reaction do exist, the resulting rovibrational distribution of NO is not known. A determination of the underlying potential energy surfaces will facilitate such calculations.

Acknowledgments

This work was supported in part by the National Science Foundation, Division of Atmospheric Science.

References

[1] M. Ahmadjian, R.M. Nadile, and J. O. Wise, J. Spacecraft Rockets 27 (1990) 66.

[2] D. R. Smith and M. Ahmadjian, Geophys. Res. Lett. 20 (1993) 2679.

[3] Ya. B. Zeldovich, P. Ya. Sadovnikov, and D.A. Frank-Kamenetskii, *Oxidation of Nitrogen in Combustion*, Academy of Sciences of the USSR, Institute for Chemical Physics, Moscow-Leningrad (translated by M. Shelef), 1947.

[4] R. D. Sharma, Y. Sun, and A. Dalgarno, Geophys. Res. Lett. 20 (1993) 2043.

[5] P. K. Swaminathan, D. F. Strobel, D. G. Kupperman, C. Krishna Kumar, L. Acton, R. DeMajistre, J.-H. Yee, L. Paxton, D. E. Anderson, D. J. Strickland, and J. W. Duff, J. Geophys. Res. 103 (1998) 11579.

[6] N. Balakrishnan, E. Sergueeva, V. Kharchenko, and A. Dalgarno, J. Geophys. Res. 105 (2000) 18549.

[7] C. T. Bowmann, Combustion Sci. and Tech. 3 (1971) 37.

[8] D. L. Baulch, D. D. Drysdale, and D. G. Haine, *Evaluated Kinetic Data for High Temperature Reactions*, Butterworths, London, 1973; Vol. 2.

[9] D. L. Baulch, C. J. Cobos, R. A. Cox, G. Hayman, Th. Just, J. A. Kerr, T. Murrells, M. J. Pilling, J. Troe, R. W. Walker, and J. Warnatz, J. Phys. Chem. Ref. Data 23 (1994) 873.

[10] M. E. Whitson Jr., L. A. Darnton, and R. J. McNeal, Chem. Phys. Lett. 41 (1976) 552.

[11] A. Rahbee and J. J. Gibson, J. Chem. Phys. 74 (1981) 5143.

[12] R. R. Herm, B. J. Sullivan, and M. E. Whitson Jr., J. Chem. Phys. 79 (1983) 2221.

[13] I. C. Winkler, R. A. Stachnik, J. I. Steinfeld, and S. M. Miller, J. Chem. Phys. 85 (1986) 890.

[14] G. E. Caledonia, R. H. Krech, D. B. Oakes, S. J. Lipson, and W. A. M. Blumberg, J. Geophys. Res. 105 (2000) 12833.

[15] M. Gilibert, A. Aguilar, M. González, and R. Sayós, Chem. Phys. 172 (1993) 99; 178 (1993) 287.

[16] J. W. Duff, F. Bien, and D. E. Paulsen, Geophys. Res. Lett. 21 (1994) 2043.

[17] M. Gilibert, X. Giménez, M. González, R. Sayós, and A. Aguilar, Chem. Phys. 191 (1995) 1.

[18] G. Suzzi, R. Orrú, E. Clementi, A. Lagana, and S. Crocchianti, J. Chem. Phys. 102 (1995) 2825.

[19] D. Bose and G. V. Candler, J. Chem. Phys. 107 (1997) 6136.

[20] R. Sayós, J. Hizago, M. Gilibert, and M. González, Chem. Phys. Lett. 284 (1998) 101.

[21] N. Balakrishnan and A. Dalgarno, Chem. Phys. Lett. 302 (1999) 485.

[22] S. P. Walch and R. L. Jaffe, J. Chem. Phys. 86 (1987) 6946.

[23] J. C. Polanyi, Acc. Chem. Res. 5 (1972) 161.

[24] J. P. Kennealy, F. P. Del Greco, G. E. Caledonia and B. D. Green, J. Chem. Phys. 69 (1978) 1574.

[25] B. D. Green, G. E. Caledonia, W. A. M. Blumberg and F. H. Cook, J. Chem. Phys. 89 (1984) 773.

[26] W. T. Rawlins,M. E. Fraser and S. M. Miller, J. Phys. Chem. 93 (1989) 1097.

[27] See Table 2 of Ref. [14].

Table I. Comparison of selected results from the present calculations with the experimental results of Caledonia et al. [14] and the calculations of Duff [27].

v'	$j_{\max}$	$\langle j' \rangle$	$T_{rot}(\langle j' \rangle)$ (K)	$\sigma_{v'}(\mathring{A}^2)/\pi$ This work	$\sigma_{v'}(\mathring{A}^2)/\pi$ Ref. [14]	$\sigma_{v'}(\mathring{A}^2)/\pi$ Duff [27]	$\sigma_{v'}^{v=0}(\mathring{A}^2)/\pi$ This work
0	155	118	17221	0.28	-	-	0.24
1	151	110	14975	0.41	0.49	0.37	0.38
2	147	104	13393	0.46	0.65	0.42	0.42
3	144	100	12387	0.44	0.20	0.39	0.40
4	139	97	11659	0.37	0.69	0.36	0.34
5	137	93	10722	0.32	0.37	0.31	0.29
6	133	90	10045	0.28	0.20	0.27	0.25
7	130	87	9390	0.24	0.25	0.23	0.21
8	126	83	8551	0.22	-	-	0.19
9	121	79	7751	0.18	-	-	0.16
10	118	76	7177	0.14	-	-	0.11
11	112	74	6807	0.11	-	-	0.09
12	109	70	6096	0.08	-	-	0.07
13	103	66	5423	0.07	-	-	0.06
14	98	62	4791	0.06	-	-	0.05
15	92	58	4197	0.04	-	-	0.04
16	85	54	3643	0.04	-	-	0.03
17	80	53	3510	0.03	-	-	0.02
18	78	47	2767	0.02	-	-	0.02

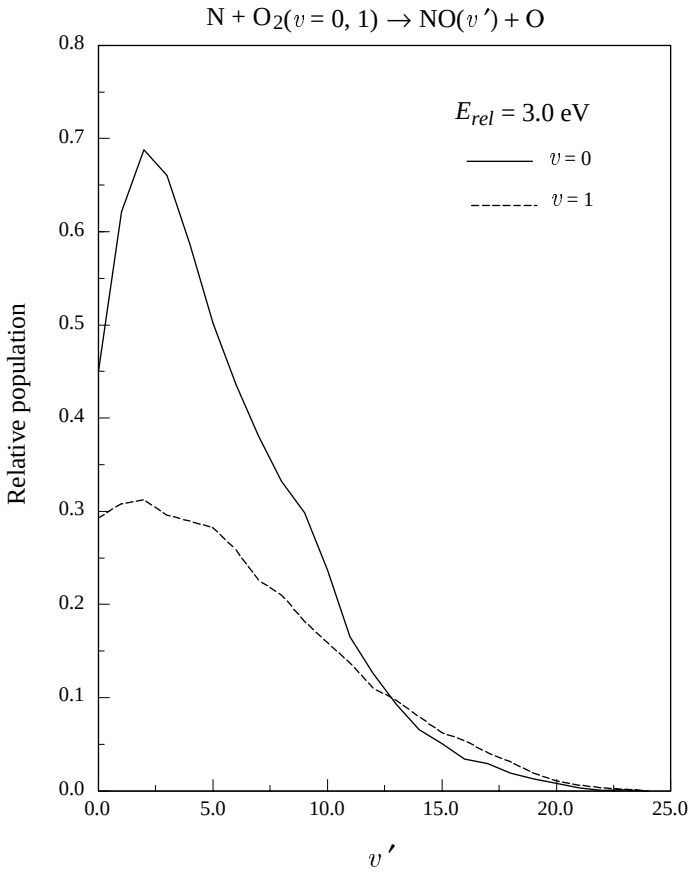

Figure 1: Product vibrational distributions at $E_{rel} = 3.0$ eV. The O_2 rotational temperature is assumed to be 1000 K.

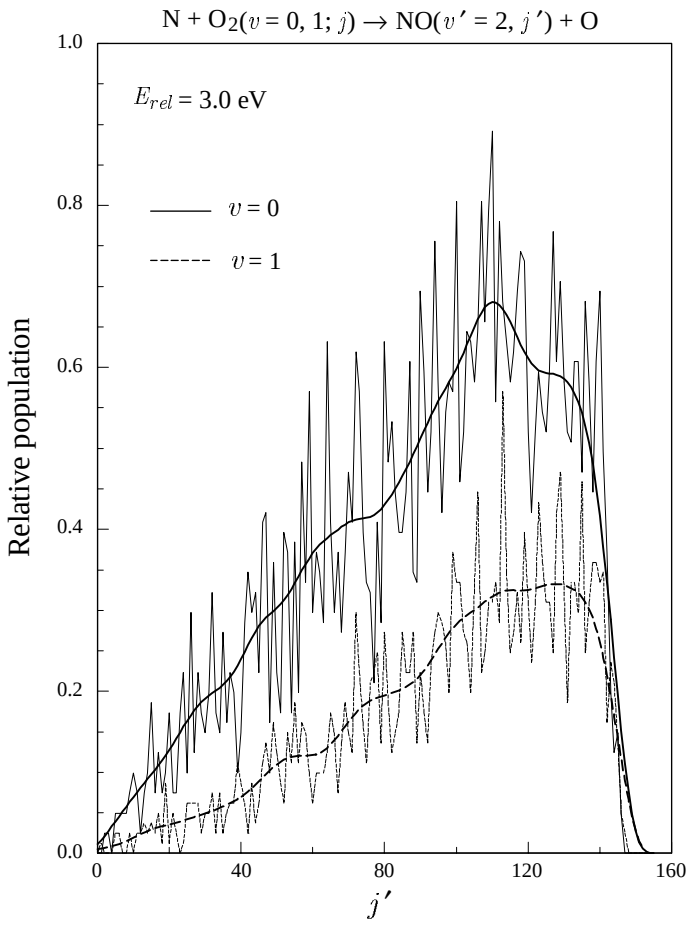

Figure 2: Product rotational distribution in NO($v' = 2$) from N + O_2($v = 0, 1$) collisions at a collision energy of 3.0 eV. The reactant rotational temperature is 1000 K. The smoother lines represent smoothed distributions using Gaussians of HWHM = 5 (see text).

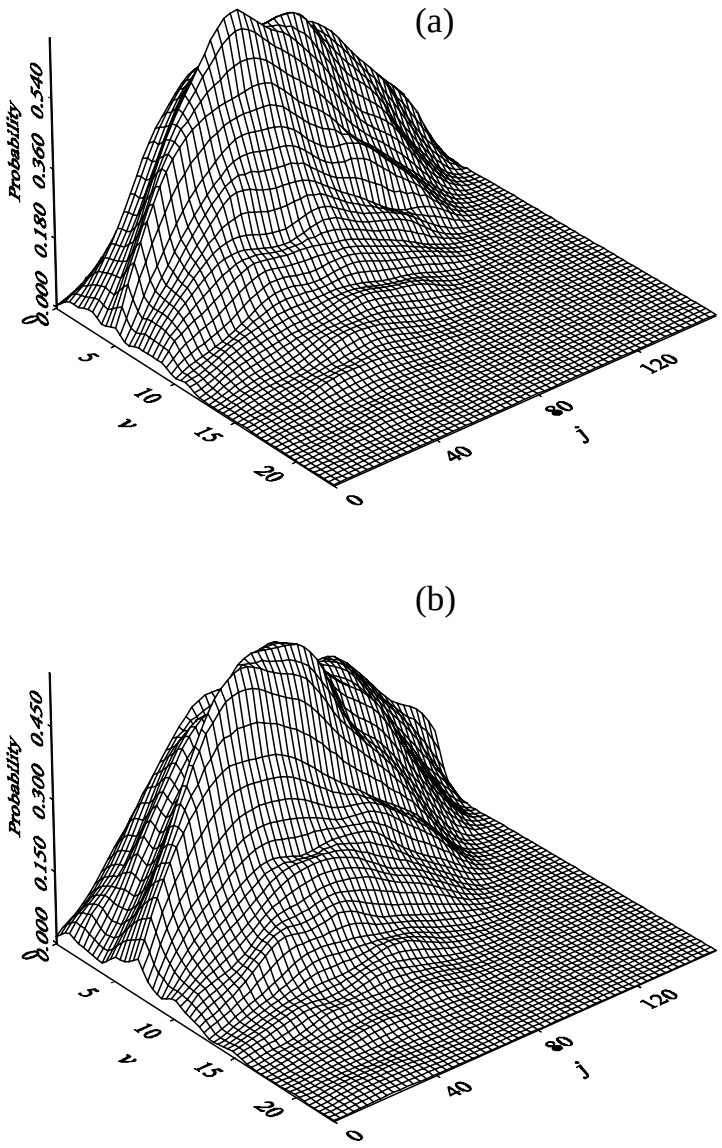

Figure 3: Product rovibrational distributions from N + O_2 reactive collisions corresponding to a reactant rotational temperature of 742 K, over a range of collision energies from 0.30 to 3.0 eV. (a) Distribution resulting from the O_2 $v = 0$ state, and (b) distribution resulting from the O_2 $v = 1$ state.

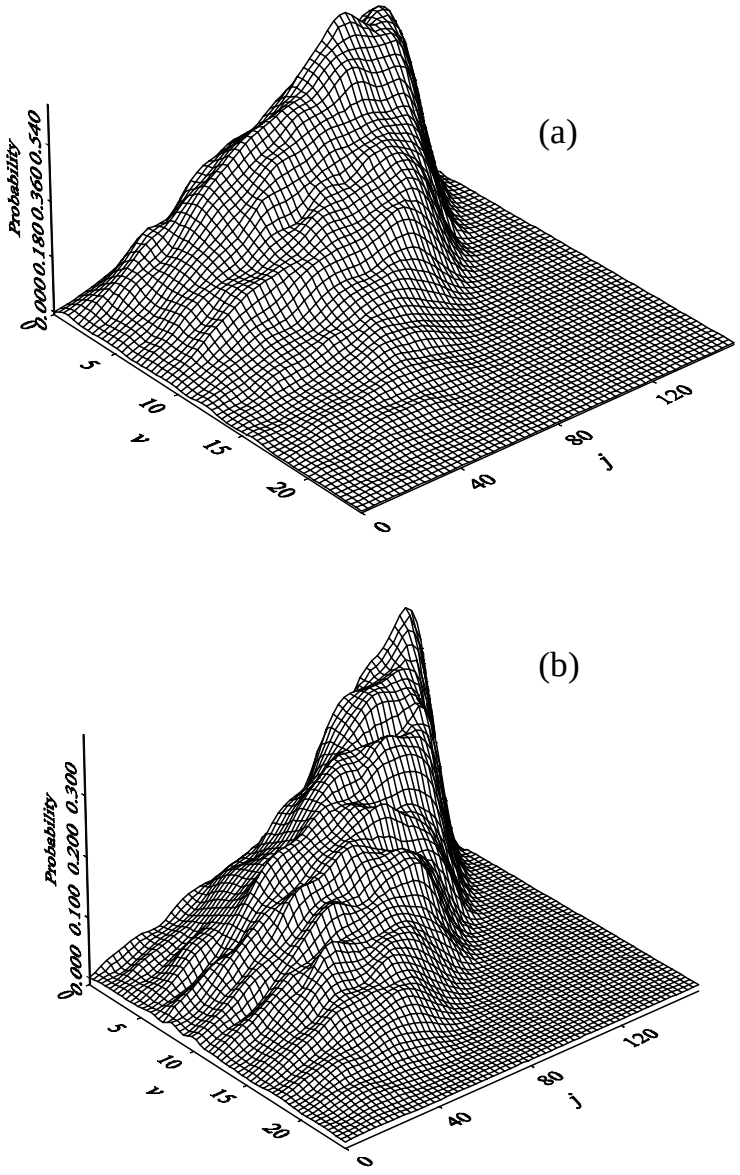

Figure 4: Same as Fig. 3, but for the fixed collision energy of 3.0 eV and O_2 rotational temperature of 1000 K.

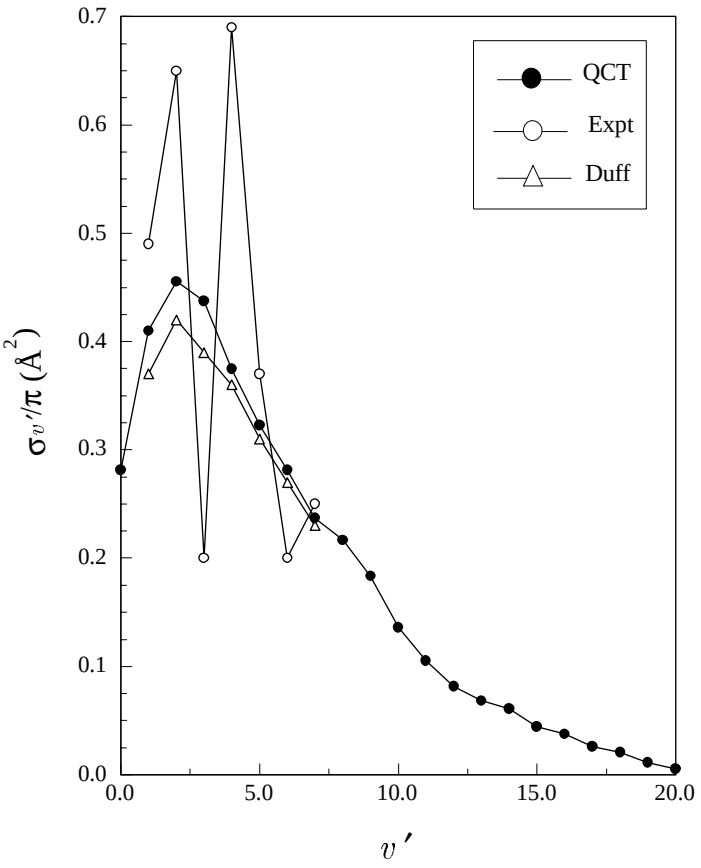

Figure 5: Comparison of the experimental [14] cross sections for $N + O_2(v = 0, 1) \rightarrow NO(v') + O$ with the results of the present calculations and those of Duff [27].